

Two independent pathways of regulated necrosis mediate ischemia–reperfusion injury

Andreas Linkermann^a, Jan Hinrich Bräsen^{b,c}, Maurice Dardigny^d, Mi Kyung Jin^a, Ana B. Sanz^e, Jan-Ole Heller^a, Federica De Zen^a, Ricardo Weinlich^f, Alberto Ortiz^e, Henning Walczak^d, Joel M. Weinberg^g, Douglas R. Green^f, Ulrich Kunzendorf^{a,1}, and Stefan Krautwald^a

^aDivision of Nephrology and Hypertension and ^bInstitute for Pathology, Christian-Albrechts-University, 24105 Kiel, Germany; ^cPathology Hamburg-West, Institute for Diagnostic Histopathology and Cytopathology, 22767 Hamburg, Germany; ^dCell Death and Inflammation Laboratory, Centre for Cell Death, Cancer and Inflammation, University College London Cancer Institute, London WC1E 6BT, United Kingdom; ^eEl Instituto de Investigación Sanitaria de la Fundación Jiménez Diaz, Redínren, Fundación Renal Íñigo Álvarez de Toledo, Universidad Autónoma de Madrid, 28049 Madrid, Spain; ^fDepartment of Immunology, St. Jude Children's Research Hospital, Memphis, TN 38105-3678; and ^gDivision for Nephrology, University of Michigan Medical Center, Ann Arbor, MI 48109-5676

Edited* by Tak W. Mak, The Campbell Family Institute for Breast Cancer Research, Ontario Cancer Institute at Princess Margaret Hospital, University Health Network, Toronto, Canada, and approved June 3, 2013 (received for review March 25, 2013)

Regulated necrosis (RN) may result from cyclophilin (Cyp)D-mediated mitochondrial permeability transition (MPT) and receptor-interacting protein kinase (RIPK1)-mediated necroptosis, but it is currently unclear whether there is one common pathway in which CypD and RIPK1 act in or whether separate RN pathways exist. Here, we demonstrate that necroptosis in ischemia–reperfusion injury (IRI) in mice occurs as primary organ damage, independent of the immune system, and that mice deficient for RIPK3, the essential downstream partner of RIPK1 in necroptosis, are protected from IRI. Protection of RIPK3-knockout mice was significantly stronger than of CypD-deficient mice. Mechanistically, *in vivo* analysis of cisplatin-induced acute kidney injury and hyperacute TNF-shock models in mice suggested the distinctness of CypD-mediated MPT from RIPK1/RIPK3-mediated necroptosis. We, therefore, generated CypD-RIPK3 double-deficient mice that are viable and fertile without an overt phenotype and that survived prolonged IRI, which was lethal to each single knockout. Combined application of the RIPK1 inhibitor necrostatin-1 and the MPT inhibitor sanglifehrin A confirmed the results with mutant mice. The data demonstrate the pathophysiological coexistence and corelevance of two separate pathways of RN in IRI and suggest that combination therapy targeting distinct RN pathways can be beneficial in the treatment of ischemic injury.

RIP3 | RIP1 | programmed necrosis | apoptosis

Unlike apoptosis, necrosis was considered to be an accidental form of cell death until genetically determined, regulated processes that mediate necrotic cellular demise were identified *in vivo* (1, 2). Histologically, the majority of cellular damage in renal and other forms of ischemia–reperfusion injury (IRI) is caused by necrosis (3, 4). With the recognition of regulated necrosis (RN), the intriguing opportunity to pharmacologically interfere with these pathways has emerged. RN can be mediated by mitochondrial permeability transition (MPT), a process that critically depends on the protein cyclophilin (Cyp)D (5,6,7,8). The MPT has been successfully modified in patients with myocardial infarction (9) and is recognized as the major regulated necrotic signal from mitochondria (6). Receptor-interacting protein (RIP) kinase (RIPK1)-mediated necroptosis contributes to the pathogenesis in preclinical models of brain, heart, and kidney IRI (10–12) and was demonstrated to result in the rapid, active, and dynamic release of cell death associated molecular patterns (CDAMPs) following loss of plasma membrane integrity, a process that strongly attracts immune cells (13, 14) and promotes ongoing secondary injury. Necroptosis occurs as a consequence of death receptor signaling upon formation of the RIPK1/RIPK3/mixed lineage kinase domain-like (MLKL)-containing necrosome (1, 15). The relevance of necroptosis has been clearly demonstrated by the reversal of the lethal phenotype of caspase-8-deficient mice on a RIPK3-knockout

(ko) background (16, 17). Necroptosis is now understood as a second-line defense mechanism of the host to defend viruses that express inhibitors of caspase-8 (15, 18, 19, 20), which some viruses bypass by additionally expressing inhibitors that prevent the cross-phosphorylation of RIPK1 and RIPK3 (21, 22), a process that is required for necroptosis and depends on the RIP homotypic interaction motif (RHIM) domain (23, 24). At least for the kidney, it appears that necroptosis predominates over apoptosis and similar suggestions have been made in myocardial IRI (11, 25). However, existing data that imply protection by interference with necroptosis in various *in vivo* models used the RIPK1 kinase inhibitor necrostatin (Nec)-1 to inhibit necrotic signaling (10, 11, 26, 27). However, Nec-1 has recently been discussed to directly influence the immune system, besides its effects to block release of CDAMPs (28, 29). Therefore, it remains an open question whether necroptosis in IRI is of relevance in the absence of a functional immune system.

Regulated necrosis is not restricted to MPT-induced RN and necroptosis because ferroptosis (30), pyroptosis (31, 32), poly(ADP-ribose)-polymerase 1 (PARP1)-mediated regulated necrosis (6), and others have been identified (33). It is currently unclear how RN pathways are interconnected and whether targeted or pharmacological interference with more than one pathway might be of additional benefit. Here, we demonstrate that RIPK3-ko mice are protected from IRI and that protection from inhibition with necroptosis also occurs in immunodeficient SCID-Beige mice that were treated with Nec-1. We further provide several lines of *in vivo* and *in vitro* evidence for the clear separation of necroptosis from MPT-mediated RN, including studies with newly developed CypD/RIPK3 double-deficient mice that demonstrate striking protection from prolonged ischemia periods. Pharmacological inhibition of MPT by sanglifehrin (Sf)A and necroptosis by Nec-1 confirmed these results, which strongly suggest combination therapy to be beneficial for the prevention of IRI.

Results

We generated CypD-RIPK3 double-deficient mice, which did not exhibit an overt phenotype in any of the investigated organs

Author contributions: A.L., A.O., H.W., J.M.W., D.R.G., U.K., and S.K. designed research; A.L., J.H.B., M.D., M.K.J., A.B.S., J.-O.H., F.D.Z., R.W., J.M.W., and S.K. performed research; A.O. and D.R.G. contributed new reagents/analytic tools; A.L., J.H.B., M.D., H.W., J.M.W., D.R.G., U.K., and S.K. analyzed data; A.L. and D.R.G. wrote the paper; and A.L. and S.K. supervised double-knockout crosses.

The authors declare no conflict of interest.

*This Direct Submission article had a prearranged editor.

¹To whom correspondence should be addressed. E-mail: kunzendorf@nephro.uni-kiel.de.

This article contains supporting information online at www.pnas.org/lookup/suppl/doi:10.1073/pnas.1305538110/-DCSupplemental.

(Fig. S1 A–C). To avoid the presence of collateral vessels, which are known to influence the readout systems in myocardial ischemia and stroke models, we focused on a renal model of IRI that is lethal to wild-type (wt) mice after ~72 h following reperfusion to investigate the CypD-RIPK3 double-knockout (dko) mice in comparison with wt, RIPK3-ko, and CypD-ko mice (Fig. 1A). Whereas CypD-deficient mice and RIPK3-ko mice exhibited significantly prolonged survival in this model ($P < 0.01$ and < 0.001 , respectively), but died after no longer than 120 h, all investigated CypD-RIPK3-dko mice survived long term ($P < 0.001$ in comparison with all other groups). In line with this finding, markers for the loss of kidney function (elevated serum concentrations of creatinine and urea) were significantly reduced 48 h after reperfusion in CypD-ko mice and RIPK3-ko mice, but the strongest protection was again seen in the CypD-RIPK3-dko mice (Fig. 1 D and E). Histological analysis revealed significant reduction of kidney damage in all ko and dko mice, with the strongest protection again noted for the CypD-RIPK3-dko mice (Fig. 1 B and C). However, significantly increased organ damage was still observed in the CypD-RIPK3-dko mice compared with sham-treated mice (Fig. 1 B and C).

To investigate the role of necroptosis in the kidney in more detail, we examined the expression levels of regulators of cell

death in renal lysates from IRI-treated mice. Expression of the survival parameter p38 (34) and the RIPK1 regulator SHARPIN revealed a role of this system in the time-course of IRI (Fig. S2). Cleaved caspase-3 was not detectable in kidney lysates within the ischemic period and over the first 96 h after reperfusion (Fig. S2), indicating that cell death was not apoptotic. In addition, changes in expression of RIPK1 in the renal tubules 48 h after reperfusion were analyzed by immunohistochemistry, demonstrating subcellular changes in the expression profile (Fig. S3 A and B). In whole-kidney lysates, RIPK1 expression appeared to slightly increase upon ischemia in both wt and RIPK3-deficient mice (Fig. 2A) but was slightly down-regulated between 2–8 h after the beginning of reperfusion. We failed to clearly detect RIPK3 expression in the renal lysates, most probably because of overall low expression levels in the kidney. To further understand the role of necroptosis in the kidney, we assessed the in vivo model of cisplatin-induced acute kidney injury (CP-AKI) (35), which we found to be attenuated by Nec-1 (Fig. S3 C–E). In line with our previous suggestion that death receptor-mediated apoptosis is of minor pathophysiological importance in kidney IRI (11), and to further investigate the in vivo relevance of necroptosis beyond the use of Nec-1, we compared RIPK3- to caspase-8–RIPK3 double-deficient mice in a standard renal IRI model. As expected from Fig. 1A, RIPK3-ko mice were protected from IRI, but no additive protection was recognized for the caspase-8–RIPK3-dko mice (Fig. 2 B–E). This result is in line with the absence of cleaved caspase-3 in the time course of IRI (Fig. S2D). It was suggested that the protective effect of CypD is most significant in a mild model of IRI (36). Therefore, to precisely define the relative contribution of RN mediated by CypD and RIPK3 to the overall damage in IRI, we reduced the duration of the ischemic phase and directly compared wt mice, CypD-ko mice and RIPK3-ko mice. Clearly, the level of protection from mild kidney IRI was significantly stronger in RIPK3-ko mice compared with CypD-ko mice (Fig. 2 F–I).

Having delineated the in vivo role of necroptosis in IRI, we next aimed to pharmacologically inhibit necroptosis by using a previously described inhibitor of the kinase activity of RIPK1, Nec-1 (10, 26). However, Nec-1 is also known to inhibit indoleamine-2,3-dioxygenase (IDO), which means that it can exert effects on the immune system that are independent of the inhibition of the kinase activity of RIPK1 (28, 37). To circumvent IDO inhibition-mediated effects of Nec-1 on the immune cells, we used freshly isolated renal tubules and immunodeficient SCID-Beige mice. In renal proximal tubular cells, we found that application of tumor necrosis factor (TNF), TNF-related weak inducer of apoptosis (TWEAK), and IFN- γ , referred to as the TTI model, resulted in caspase-independent cell death (CICD), as reported previously (38), which we here identified as necroptosis by the addition of Nec-1 (Fig. S4 A–D). Consistent with previous concepts of necroptosis (1, 39), addition of the pan-caspase inhibitor zVAD-fmk (zVAD) shifted apoptotic cell death to necroptosis (Fig. S4 B and D). We applied the TTI model in murine freshly isolated wt tubules and performed TUNEL staining, a nonspecific marker that detects double-strand breaks that are produced during apoptosis but can also arise from the action of nucleases during necrotic death (40) and detected TUNEL-positive cells after combined application of TTI and zVAD. Addition of Nec-1 reduced the number of TUNEL-positive cells to the level of control tubules, thereby identifying this CICD as necroptosis (Fig. 3 A and B; higher magnification is provided in Fig. S5). In immunodeficient SCID-Beige mice, we investigated kidney IRI in the presence and absence of Nec-1. Analysis of histopathological staining of representative kidney sections revealed significant protection upon the use of Nec-1 (Fig. 3 C and D) and prevention of the associated increase in serum creatinine and serum urea levels (Fig. 3 E and F). We then isolated renal tubules from RIPK3-deficient

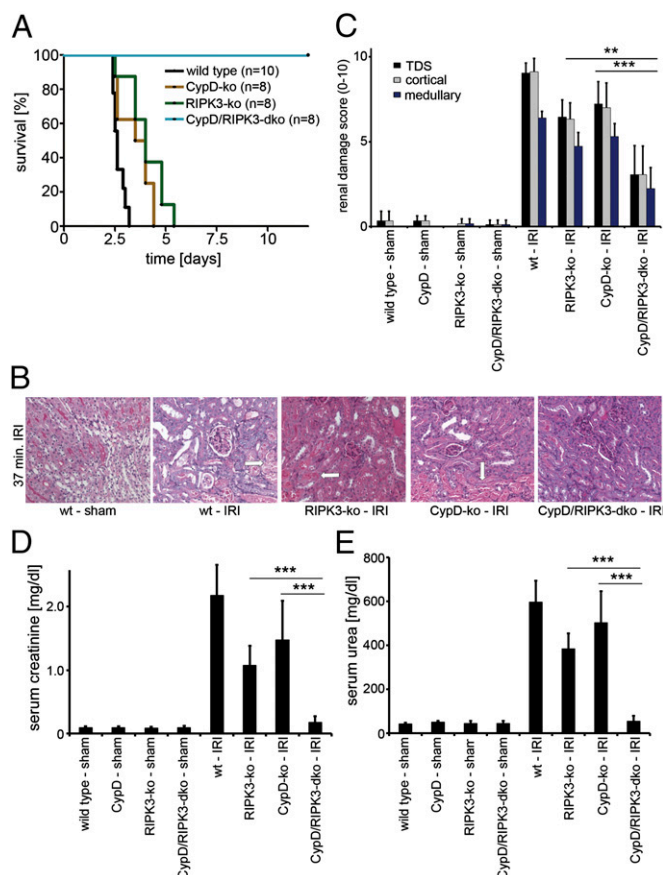


Fig. 1. Increased protection from ischemia-reperfusion damage by combined loss of RIPK3 and CypD. Mice underwent severe renal IRI. (A) Survival proportions of indicated mice following IRI. (B) Representative periodic acid-Schiff (PAS)-stained histomicrographs of mice with indicated genotype 48 h after severe IRI. White arrows point to typical necrotic changes classically observed in proximal tubules upon renal IRI. (C) Quantification by renal damage score of B. (D and E) Serum creatinine and serum urea concentrations 48 h following reperfusion or sham operation. ** $P < 0.01$; *** $P < 0.001$ ($n = 8$ –12 per group).

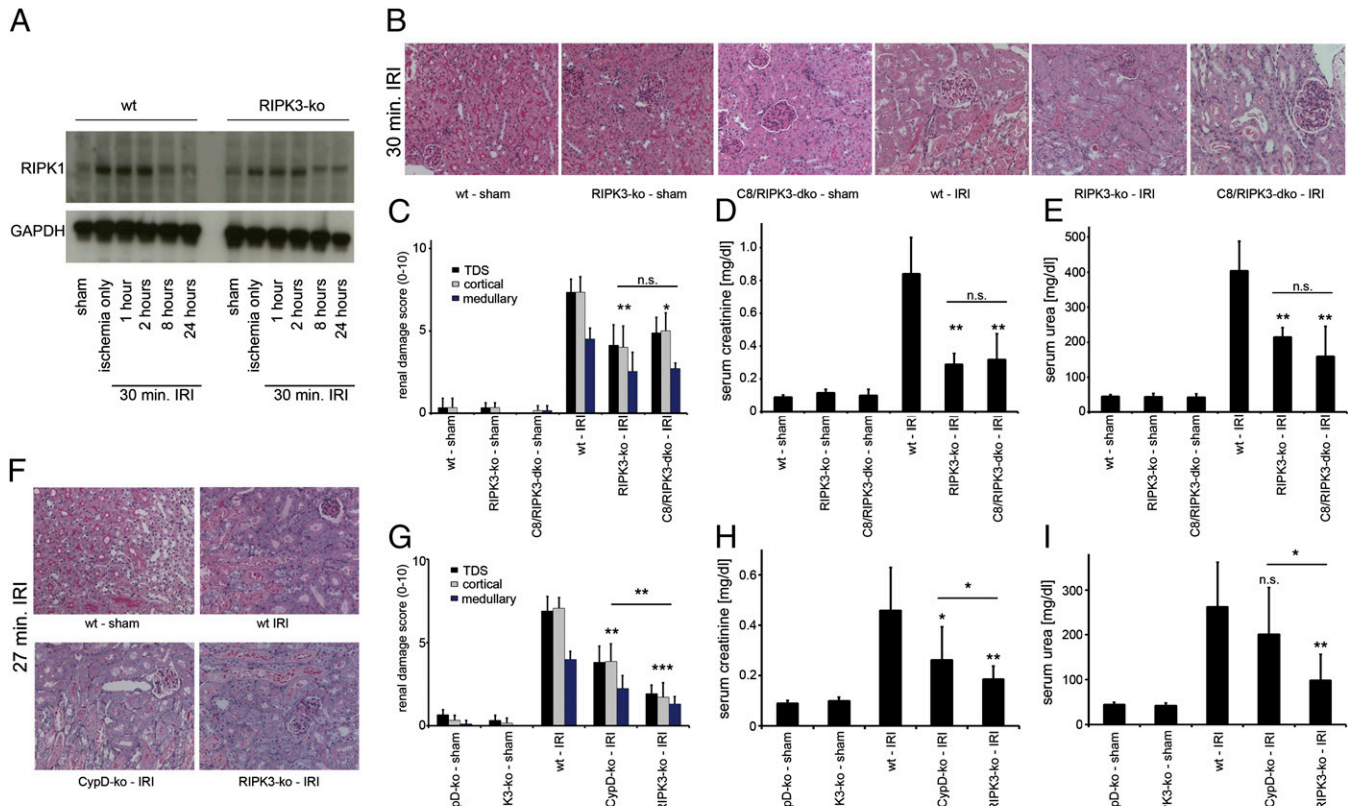


Fig. 2. RIPK3 and CypD contribute to ischemia–reperfusion damage but caspase-8 does not. (A) Expression levels of RIPK1 in whole-kidney lysates taken from wt or RIPK3-ko mice during the time course of IRI in wt mice. GAPDH serves as a loading control. (B) wt, RIPK3-ko, and caspase-8 (C8)/RIPK3-dko mice underwent renal IRI 48 h before preparation of PAS-stained renal sections and its quantification using the renal damage score (C). (D and E) Corresponding serum creatinine and serum urea concentrations 48 h after reperfusion ($n = 8$ –12 per group). (F–I) Comparison of wt, CypD-ko, and RIPK3-ko mice in a mild IRI setting ($n = 7$ –16 per group).

mice that showed ex vivo protection from hypoxia–reoxygenation, as evaluated by lactate dehydrogenase (LDH) release and propidium iodide (PI) positivity (Fig. 3 G and H). From these data, we conclude that kidney cells readily undergo necroptosis and the prevention of necroptosis by Nec-1 is independent of the immune system.

To confirm that CypD-mediated MPT and RIPK3-mediated RN display two distinct RN pathways, we provide four further lines of evidence. First, whereas Nec-1 protected L929 cells from death in a standard model of TNF/zVAD-induced necroptosis, the MPT inhibitor SfA did not exhibit any protective effects (Fig. S6A), and, conversely, Nec-1 did not protect Jurkat cells in standard model of MPT pore opening, whereas SfA did (Fig. S6B). Second, as demonstrated above, in the model of cisplatin-induced AKI, RIPK3-ko mice, despite a significant protection compared with wt mice, did not reach the level of protection seen in CypD-ko mice (Fig. S7A). Third, in cisplatin-induced AKI, whereas RIPK3-ko mice survived significantly longer in the presence of zVAD or on caspase-8-deficient background (Fig. S7B), any combination of zVAD and Nec-1 or the combined CypD-RIPK3 double-deficient background did not prolong survival of CypD-ko mice (Fig. S6C). Fourth, RIPK3-deficient, but not CypD-deficient, mice were protected from hyperacute TNF-induced shock (41, 42) (Fig. S8). These lines of evidence led us to conclude that CypD-mediated RN and necroptosis are two distinct pathways of RN. To pharmacologically interfere with both of these pathways, we first confirmed the pathway specificity of Nec-1 for necroptosis and SfA for CypD-mediated RN by applying Nec-1 in RIPK3-deficient mice and SfA in

CypD-deficient mice, and no significant differences in organ damage were recognized (Fig. S9). As demonstrate in Fig. 4 A and B, no additional protection compared with the one described in Fig. 4 D and E for the single-ko mice was detected when inhibitors were applied correspondingly. In contrast, when we applied combination therapy of Nec-1 and SfA 15 min before ischemia in the severe kidney IRI model into wt mice, a significant survival benefit was detected compared with mice treated with Nec-1 or SfA alone (Fig. 4C). The superior therapeutic effect of the Nec-1/SfA combination was also detected by a marked reduction in serum creatinine and serum urea concentrations (Fig. 4 F and G) and upon histological evaluation of kidneys harvested 48 h after reperfusion (Fig. 4 D and E). Even though the protection from kidney damage upon long ischemia afforded by combined application of Nec-1 and SfA before reperfusion was substantial, it was not complete suggesting the involvement of other pathways of regulated necrosis.

Discussion

The parallel existence of two pathways that induce regulated necrosis in the same organ following the same ischemic stimulus demonstrates the complexity in the pathophysiology of IRI. Whereas intracellular changes in pH and lipid peroxidation may favor necrosis as a result of MPT (1, 6), necroptosis is triggered by stimulation of death receptors and controlled by regulatory inhibitors, most prominently by the polyubiquitination of RIPK1, which is mediated by cellular inhibitor of apoptosis (43) and the linear ubiquitin chain assembly complex (LUBAC) (44). Independently of these considerations, concomitant application of Nec-1 and SfA prevents both of these pathways from inducing

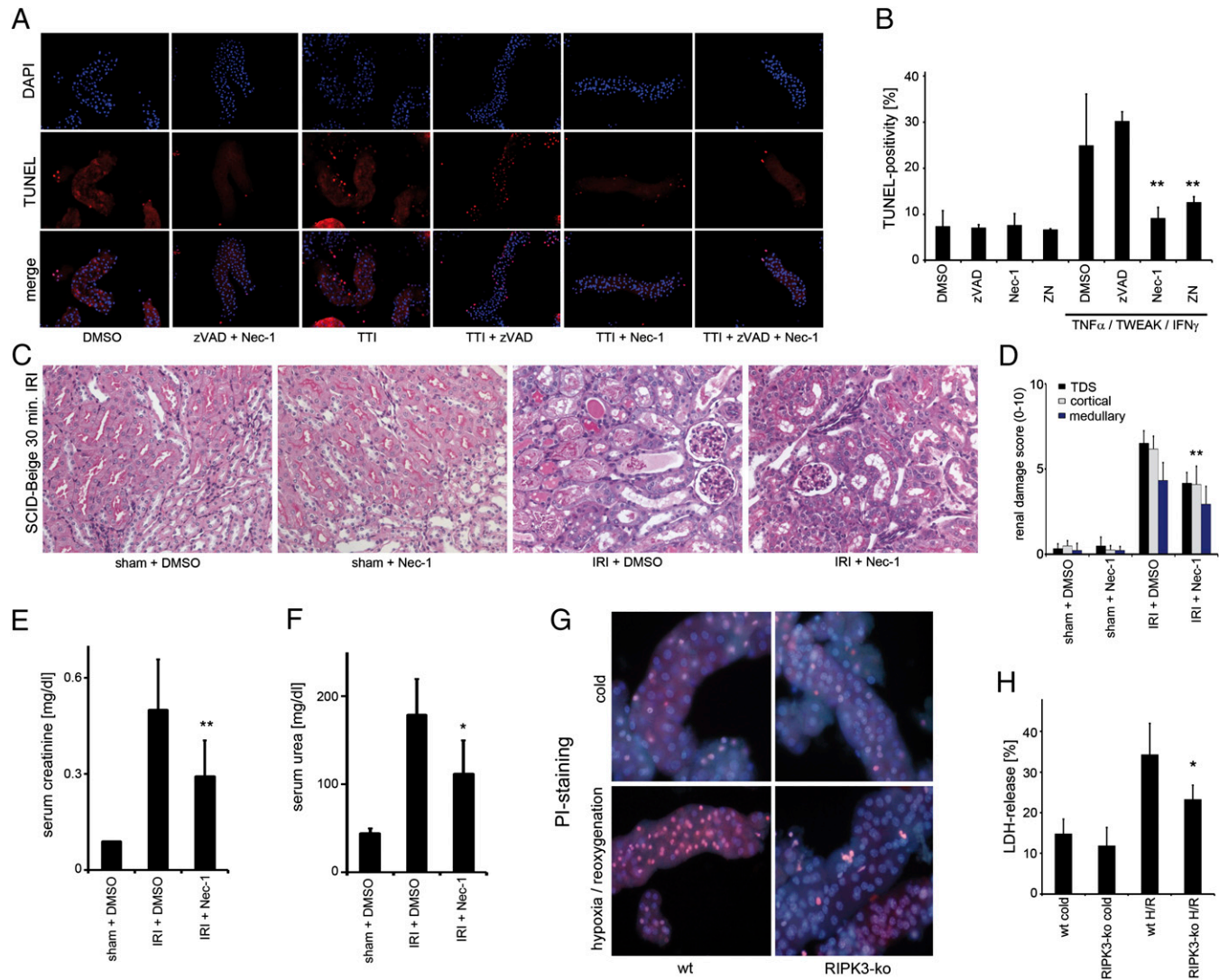


Fig. 3. Necroptosis occurs independently of the immune system. (A) Freshly isolated renal tubules were treated for 6 h after preparation with indicated agents before assessment of TUNEL positivity and quantification (B). (C and D) Representative PAS-stained kidney sections (C) and evaluation of renal damage (D) from SCID-Beige mice that underwent ischemia–reperfusion in the presence of DMSO or Nec-1. Corresponding serum concentrations of creatinine (E) and urea (F) are shown 48 h after reperfusion ($n = 8$ per group). (G) PI staining of freshly isolated renal tubules from wt or RIPK3-ko mice that underwent 60 min of hypoxia followed by 60 min of reperfusion. (H) LDH-release assay of the similar tubules as in G.

cell death upon ischemia–reperfusion and, thereby, appears to provide a previously unreached level of protection from IRI. The strong additive benefit of CypD- and RIPK3-ko in the present studies raises the interesting question of whether mice deficient in more than two RN pathways would be further protected. Because all injury is not prevented in the CypD-RIPK3 dko and the absence of the RN pathways is well tolerated under physiological conditions, future work along these lines is both feasible and potentially highly informative.

The importance of necroptosis suggested by the earlier work with Nec-1, and conclusively shown in the present studies with the mutant mouse model, raises the question as to what triggers necroptosis in tubular cells. TNF receptor 1/2 double-deficient mice are not protected from renal IRI, and interference with TNF does not protect mice from IRI (45). However, other members of the TNF superfamily have recently been implicated in the induction of necroptosis [e.g., TNF related apoptosis inducing ligand receptor (TRAIL-R) (46), Fas, or TWEAK] and are just as likely to be involved as members of the Toll-like receptors, some of which may trigger the intracellular RHIM-containing

protein TRIF (TIR-domain-containing adapter-inducing interferon- β) (16). Our data (Fig. 3A) implicate a role for the TWEAK/FN14 system, at least in isolated renal tubules.

The absence of an overt phenotype in the CypD/RIPK3-dko mice contrasts with the early lethality and tumor susceptibility usually seen in mutant mice lacking major central pathways of apoptosis (16, 47, 48) and indicates the predominant involvement of RN mechanisms in severe stress and injury settings as opposed to the physiologic role of apoptosis during development, adult tissue remodeling, and immune system regulation. A similar distinction holds true for at least two of the other RN pathways, pyroptosis (31) and parthanatos (49), because caspase-11-deficient mice that do not undergo pyroptosis and PARP1-deficient mice that do not undergo parthanatos are also viable and fertile. An increasing number of RN pathways have recently been described, including MPT, necroptosis, pyroptosis, ferroptosis (30, 50), heat stroke-associated cell death (33), direct lysosomal membrane permeabilization (51), etc., but the complex regulation and interconnectivity among these RN pathways is not understood today.

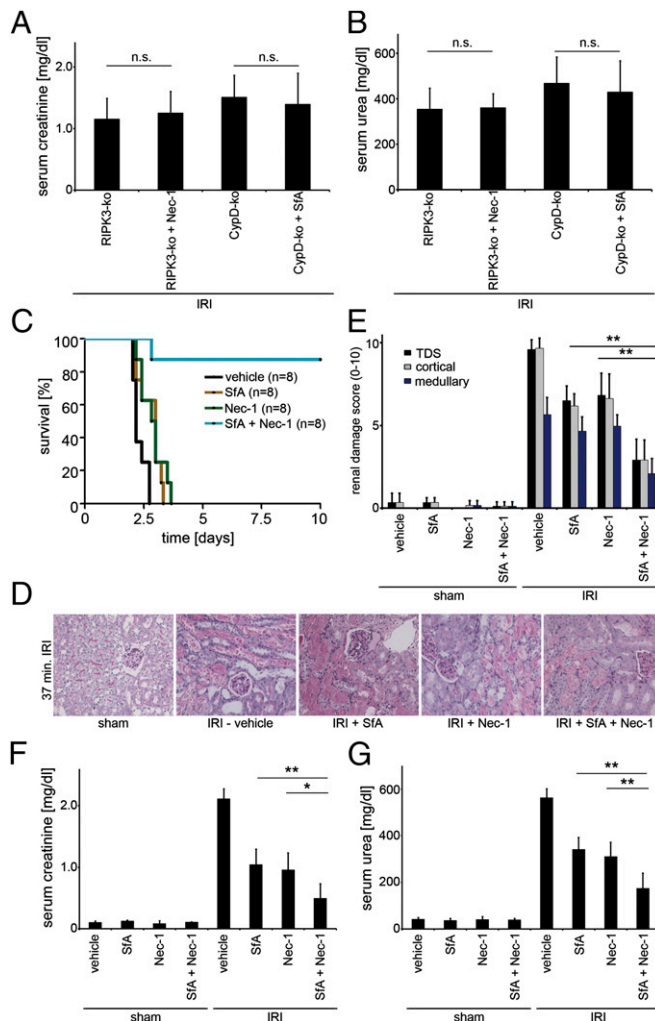


Fig. 4. Combination therapy with Nec-1 and SfA provides strong protection against IRI. (A and B) RIPK3-ko and CypD-ko mice ($n = 8$ per group) underwent indicated treatment 15 min before onset of IRI surgery. Note that the neither the addition of Nec-1 to RIPK3-ko mice nor the application of SfA in CypD-ko mice led to any further protection compared with the DMSO-treated knockouts. (C–G) wt mice ($n = 8$ –12 per group) underwent indicated treatment 15 min before the onset of surgery. (C) Survival proportions following IRI. (D) Representative PAS-stained histomicrographs 48 h after severe IRI are demonstrated. (E) Quantification by renal damage score of D. (F–G) Serum creatinine and serum urea concentrations 48 h following reperfusion or sham operation. Note the additive protective effect of combination therapy. * $P < 0.05$; ** $P < 0.01$; n.s., not significant.

Targeting RN pathways depends on the availability of effective pharmacological agents, and net effects in complex disease settings are not fully predictable from expected targets. In this regard, two groups have recently reported that Nec-1 can accelerate time to death in the TNF-shock model (11, 28, 29). In the present studies, however, concomitant application of Nec-1 to modify necroptosis and SfA to modify the MPT, like the dko mice, provided marked protection from IRI. In view of the strong role played by these RN pathways, their pharmacologic modification merits further testing, particularly in transplant models that involve isolated ischemia to the organ at predictable time points and in the absence of systemic pathophysiology. Sterile tissue damage from ischemic injury that produces delayed graft function is known to play a major role in both primary non-function of the graft and as trigger for CDAMPs (13). Attempts to prevent IRI, however, face the problem that interference with RN

pathways needs to be quick within the reperfusion phase. For necroptosis, we demonstrated that applying Nec-1 fifteen minutes following reperfusion results in loss of major parts of the protective effect, which is completely absent when Nec-1 is applied 30 min after reperfusion (11), but to the best of our knowledge, the precise therapeutic window has not been investigated for other RN pathways. From a therapeutic perspective, this is disappointing because RN inhibitors might be applied too late to achieve benefits for stroke or myocardial infarction. However, the ideal application arises when IRI can be anticipated, as in solid organ transplantation or, regarding the kidney, in cardiac surgery. In these cases, protective interference with necroptosis and MPT might indeed be beneficial.

In conclusion, the present studies emphasize the importance of immunogenic cell death (52) attributable to regulated necrosis during IRI, the particular role therein of the MPT and necroptosis as independent pathways, and the additive benefit of targeting both. Further understanding of these processes and the additional pathways of regulated necrosis promises new therapeutic possibilities. In addition, IRI is known to significantly deteriorate the outcome after stroke and myocardial infarction (52, 53). Only if we precisely unravel the kinetics of the presumably narrow therapeutic window, RN-inhibiting combinatorial therapies might also provide protection in other tissues damaged by IRI.

Materials and Methods

See *SI Material and Methods* for detailed descriptions.

Reagents and Mice. Nec-1 was purchased from Sigma-Aldrich. SfA was provided by Novartis Pharma. RIPK3-deficient mice were obtained from V. Dixit (Genentech, La Jolla, CA) (54). CypD-deficient mice and SCID-Beige mice were purchased from The Jackson Laboratory, and C57BL/6 mice were from Charles River. Genotypes were confirmed by tail-snip PCR as described previously. All in vivo experiments were performed according to the *Protection of Animals Act* after approval of the German local authorities or the Institutional Animal Care and Use Committee (IACUC) of the University of Michigan and the National Institutes of Health *Guidelines for the Care and Use of Laboratory Animals* after approval from the University of Michigan IACUC. In all experiments, mice were carefully matched for age, sex, weight, and genetic background.

Mouse Models of IRI. Induction of kidney IRI was performed as described previously (11). Briefly, we performed a midline abdominal incision and a bilateral renal pedicle clamping for the indicated time using microaneurysm clamps (Aesculab). Throughout the surgical procedure, the body temperature was maintained between 37 and 38 °C by continuous monitoring using a temperature-controlled self-regulated heating system (Fine Science Tools). After removal of the clamps, reperfusion of the kidneys was visually confirmed. The abdomen was closed in two layers using standard 6-0 sutures. Sham-operated mice underwent the identical surgical procedures, except that microaneurysm clamps were not applied. To maintain fluid balance, all of the mice were supplemented with 1 mL of prewarmed PBS administered intraperitoneally directly after surgery. The mice were killed 48 h after reperfusion for each experiment. In the present study, we used mild (27 min), standard (30 min), severe (37 min), and “lethal-to-wt” (43-min) periods of ischemia before reperfusion. Mild ischemia was used for the comparison of CypD-ko mice with RIPK3-ko mice, and severe ischemia was applied to demonstrate the differences between the CypD-RIPK3 dko mice in comparison with the single-ko mice and for combination therapy in comparison with SfA or Nec-1 alone. Therefore, mice received a total volume of 200 µL of Clinoleic with or without 10 mg of SfA per kilogram of body weight and/or 1.65 mg of Nec-1 per kilogram body weight 15 min before ischemia. Serum urea and creatinine values were determined as described above. For survival experiments, mice underwent the above described procedure with 43-min bilateral renal pedicle clamping before reperfusion and were observed at least every 4–8 h for the first 7 d of the observation period.

Statistics. For all experiments, differences of data sets were considered statistically significant when P values were lower than 0.05, if not otherwise specified. Statistical comparisons were performed using the two-tailed Student *t* test. Asterisks are used in the figures to specify statistical significance (* $P < 0.05$; ** $P < 0.02$; *** $P < 0.001$).

ACKNOWLEDGMENTS. We thank V. Dixit for the RIPK3-deficient mice. We thank S. Iversen, S. Krause, M. Newsky, A. Pape, and N. F. Roeser for excellent technical support. This work is part of the MD thesis of J.-O.H. This work was funded by the German Society for Nephrology (A.L.); Novartis Pharma GmbH, Germany (A.L. and S.K.); Fresenius Medical Care, Germany (S.K. and

U.K.); INTERREG 4A Grant PN 62-1.2-10/JN 10/13123 (to U.K.); Sara Borrell and Miguel Servet FIS Contract CP12/03262 (to A.B.S.) and FIS PS09/00447 (to A.O.); RETIC REDINREN, RD12/0021/0001, Intensificación FIS-CAM, and Else Kröner-Fresenius Stiftung (to U.K.); and National Institutes of Health Grant DK34275 (to J.M.W.).

- Vandenabeele P, Galluzzi L, Vanden Berghe T, Kroemer G (2010) Molecular mechanisms of necroptosis: An ordered cellular explosion. *Nat Rev Mol Cell Biol* 11(10):700–714.
- Zhang DW, et al. (2009) RIP3, an energy metabolism regulator that switches TNF-induced cell death from apoptosis to necrosis. *Science* 325(5938):332–336.
- Bonventre JV, Weinberg JM (2003) Recent advances in the pathophysiology of ischemic acute renal failure. *J Am Soc Nephrol* 14(8):2199–2210.
- Eltzschig HK, Eckle T (2011) Ischemia and reperfusion—from mechanism to translation. *Nat Med* 17(11):1391–1401.
- Baines CP, et al. (2005) Loss of cyclophilin D reveals a critical role for mitochondrial permeability transition in cell death. *Nature* 434(7033):658–662.
- Kroemer G, Galluzzi L, Brenner C (2007) Mitochondrial membrane permeabilization in cell death. *Physiol Rev* 87(1):99–163.
- Nakagawa T, et al. (2005) Cyclophilin D-dependent mitochondrial permeability transition regulates some necrotic but not apoptotic cell death. *Nature* 434(7033):652–658.
- Schinzel AC, et al. (2005) Cyclophilin D is a component of mitochondrial permeability transition and mediates neuronal cell death after focal cerebral ischemia. *Proc Natl Acad Sci USA* 102(34):12005–12010.
- Piot C, et al. (2008) Effect of cyclosporine on reperfusion injury in acute myocardial infarction. *N Engl J Med* 359(5):473–481.
- Degterev A, et al. (2005) Chemical inhibitor of nonapoptotic cell death with therapeutic potential for ischemic brain injury. *Nat Chem Biol* 1(2):112–119.
- Linkermann A, et al. (2012) Rip1 (receptor-interacting protein kinase 1) mediates necroptosis and contributes to renal ischemia/reperfusion injury. *Kidney Int* 81(8):751–761.
- Smith CC, et al. (2007) Necrostatin: A potentially novel cardioprotective agent? *Cardiovasc Drugs Ther* 21(4):227–233.
- Kaczmarek A, Vandenabeele P, Krysko DV (2013) Necroptosis: The release of damage-associated molecular patterns and its physiological relevance. *Immunity* 38(2):209–223.
- Linkermann A, De Zen F, Weinberg J, Kunzendorf U, Krautwald S (2012) Programmed necrosis in acute kidney injury. *Nephrol Dial Transplant* 27(9):3412–3419.
- Christofferson DE, Yuan J (2010) Necroptosis as an alternative form of programmed cell death. *Curr Opin Cell Biol* 22(2):263–268.
- Kaiser WJ, et al. (2011) RIP3 mediates the embryonic lethality of caspase-8-deficient mice. *Nature* 471(7338):368–372.
- Oberst A, et al. (2011) Catalytic activity of the caspase-8-FLIP(L) complex inhibits RIPK3-dependent necrosis. *Nature* 471(7338):363–367.
- Cho YS, et al. (2009) Phosphorylation-driven assembly of the RIP1-RIP3 complex regulates programmed necrosis and virus-induced inflammation. *Cell* 137(6):1112–1123.
- Galluzzi L, et al. (2011) Molecular definitions of cell death subroutines: Recommendations of the Nomenclature Committee on Cell Death 2012. *Cell Death Differ* 19(1):107–120.
- Vandenabeele P, Vanden Berghe T, Festjens N (2006) Caspase inhibitors promote alternative cell death pathways. *Sci STKE* 2006(358):pe44.
- Upton JW, Kaiser WJ, Mocarski ES (2008) Cytomegalovirus M45 cell death suppression requires receptor-interacting protein (RIP) homotypic interaction motif (RHIM)-dependent interaction with RIP1. *J Biol Chem* 283(25):16966–16970.
- Upton JW, Kaiser WJ, Mocarski ES (2010) Virus inhibition of RIP3-dependent necrosis. *Cell Host Microbe* 7(4):302–313.
- Rebsamen M, et al. (2009) DAI/ZBP1 recruits RIP1 and RIP3 through RIP homotypic interaction motifs to activate NF-κB. *EMBO Rep* 10(8):916–922.
- Sun X, Yin J, Starovasnik MA, Fairbrother WJ, Dixit VM (2002) Identification of a novel homotypic interaction motif required for the phosphorylation of receptor-interacting protein (RIP) by RIP3. *J Biol Chem* 277(11):9505–9511.
- Kung G, Konstantinidis K, Kitsis RN (2011) Programmed necrosis, not apoptosis, in the heart. *Circ Res* 108(8):1017–1036.
- Degterev A, et al. (2008) Identification of RIP1 kinase as a specific cellular target of necrostatins. *Nat Chem Biol* 4(5):313–321.
- Northington FJ, et al. (2011) Necrostatin decreases oxidative damage, inflammation, and injury after neonatal HI. *J Cereb Blood Flow Metab* 31(1):178–189.
- Takahashi N, et al. (2012) Necrostatin-1 analogues: Critical issues on the specificity, activity and in vivo use in experimental disease models. *Cell Death Dis* 3:e437.
- Vandenabeele P, Grootjans S, Callewaert N, Takahashi N (2013) Necrostatin-1 blocks both RIPK1 and IOD: Consequences for the study of cell death in experimental disease models. *Cell Death Differ* 20(2):185–187.
- Dixon SJ, et al. (2012) Ferroptosis: An iron-dependent form of nonapoptotic cell death. *Cell* 149(5):1060–1072.
- Bergsbaken T, Fink SL, Cookson BT (2009) Pyroptosis: Host cell death and inflammation. *Nat Rev Microbiol* 7(2):99–109.
- Kayagaki N, et al. (2011) Non-canonical inflammasome activation targets caspase-11. *Nature* 479(7371):117–121.
- Kourtis N, Nikoletopoulou V, Tavernarakis N (2012) Small heat-shock proteins protect from heat-stroke-associated neurodegeneration. *Nature* 490(7419):213–218.
- Park KM, Kramer C, Vayssié-Taussat M, Chen A, Bonventre JV (2002) Prevention of kidney ischemia/reperfusion-induced functional injury, MAPK and MAPK kinase activation, and inflammation by remote transient ureteral obstruction. *J Biol Chem* 277(3):2040–2049.
- Linkermann A, et al. (2011) Renal tubular Fas ligand mediates fratricide in cisplatin-induced acute kidney failure. *Kidney Int* 79(2):169–178.
- Park JS, Pasupulati R, Feldkamp T, Roeser NF, Weinberg JM (2011) Cyclophilin D and the mitochondrial permeability transition in kidney proximal tubules after hypoxic and ischemic injury. *Am J Physiol Renal Physiol* 301(1):F134–F150.
- Kang TB, et al. (2012) Caspase-8 blocks kinase RIPK3-mediated activation of the NLRP3 inflammasome. *Immunity* 38(1):27–40.
- Sanz AB, Sanchez-Niño MD, Ortiz A (2011) TWEAK, a multifunctional cytokine in kidney injury. *Kidney Int* 80(7):708–718.
- Oberst A, Green DR (2011) It cuts both ways: Reconciling the dual roles of caspase 8 in cell death and survival. *Nat Rev Mol Cell Biol* 12(11):757–763.
- Vanden Berghe T, et al. (2013) Determination of apoptotic and necrotic cell death in vitro and in vivo. *Methods*, 10.1016/j.ymeth.2013.02.011.
- Duprez L, et al. (2011) RIP kinase-dependent necrosis drives lethal systemic inflammatory response syndrome. *Immunity* 35(6):908–918.
- Linkermann A, et al. (2012) Dichotomy between RIP1- and RIP3-mediated necroptosis in tumor necrosis factor α-induced shock. *Mol Med* 18:577–586.
- Festjens N, Vanden Berghe T, Cornelis S, Vandenabeele P (2007) RIP1, a kinase on the crossroads of a cell's decision to live or die. *Cell Death Differ* 14(3):400–410.
- Gerlach B, et al. (2011) Linear ubiquitination prevents inflammation and regulates immune signalling. *Nature* 471(7340):591–596.
- Ko GJ, et al. (2011) Blocking Fas ligand on leukocytes attenuates kidney ischemia-reperfusion injury. *J Am Soc Nephrol* 22(4):732–742.
- Jouan-Lanhouet S, et al. (2012) TRAIL induces necroptosis involving RIPK1/RIPK3-dependent PARP-1 activation. *Cell Death Differ* 19(12):2003–2014.
- Oberst A, Bender C, Green DR (2008) Living with death: The evolution of the mitochondrial pathway of apoptosis in animals. *Cell Death Differ* 15(7):1139–1146.
- Salmena L, et al. (2003) Essential role for caspase 8 in T-cell homeostasis and T-cell-mediated immunity. *Genes Dev* 17(7):883–895.
- Devalaraja Narashimha K, Padanilam BJ (2009) PARP-1 inhibits glycolysis in ischemic kidneys. *J Am Soc Nephrol* 20(1):95–103.
- Sogabe K, Roeser NF, Venkatachalam MA, Weinberg JM (1996) Differential cytoprotection by glycine against oxidant damage to proximal tubule cells. *Kidney Int* 50(3):845–854.
- Boya P, Kroemer G (2008) Lysosomal membrane permeabilization in cell death. *Oncogene* 27(50):6434–6451.
- Chen GY, Nuñez G (2010) Sterile inflammation: Sensing and reacting to damage. *Nat Rev Immunol* 10(12):826–837.
- Hotchkiss RS, Strasser A, McDunn JE, Swanson PE (2009) Cell death. *N Engl J Med* 361(16):1570–1583.
- Newton K, Sun X, Dixit VM (2004) Kinase RIP3 is dispensable for normal NF-κB signaling by the B-cell and T-cell receptors, tumor necrosis factor receptor 1, and Toll-like receptors 2 and 4. *Mol Cell Biol* 24(4):1464–1469.

Supporting Information

Linkermann et al. 10.1073/pnas.1305538110

SI Materials and Methods

Reagents and Antibodies. Necrostatin (Nec)-1 was obtained from Sigma-Aldrich. Sanglifehrin A (Sf)A was provided by Novartis Pharma. The zVAD-fmk and the recombinant purified human TNF α were purchased from BioLegend. Recombinant human TNF-related weak inducer of apoptosis (TWEAK) was from Enzo Life Sciences, and murine TNF α and murine IFN- γ were from PeproTech. The polyclonal antibody against murine receptor-interacting protein kinase (RIPK)3 was purchased from IMGENEX Biomol. Antibodies against cleaved caspase-3, GAPDH, and phospho-protein p38 (no. 9215) were purchased from Cell Signaling and New England Biolabs. The mouse α -RIPK1 antibody for Western blotting were purchased from BD Biosciences. The monoclonal SHARPIN antibody was described previously (1).

Cell Culture. L929 fibrosarcoma cells were originally obtained from ATCC and were cultured in Dulbecco's modified Eagle medium (DMEM) (Invitrogen) supplemented with 10% (vol/vol) FCS, 100 U/mL penicillin, and 100 μ g/mL streptomycin. Murine tubular epithelial (MCT) cells were cultured in RPMI 1640 (GIBCO), 10% (vol/vol) decomplemented FCS, 2 mM glutamine, 100 U/mL penicillin, and 100 μ g/mL streptomycin. All cell lines were cultured in a humidified 5% CO₂ atmosphere. For culture of tubules, Dulbecco's modified Eagle's/Ham's F-12 (DMEM-F12) without phenol red, HBSS without phenol red, calcium, magnesium, and nonessential amino acids (liquid, 100 \times) were purchased from Invitrogen. Hepes, sodium pyruvate, L-glutamine, and penicillin/streptomycin (liquid, 100 \times) were obtained from PAA Laboratories. L-Glycine was purchased from Roth. Insulin-Transferrin-Sodium Selenite Supplement was obtained from Roche Diagnostics. Collagenase class 2 was obtained from Biochrom. The 250- μ m nylon sieve was purchased from Thermo Scientific, and the 100- μ m nylon sieve was from BD Biosciences.

Mice. Eight- to twelve-week-old male C57BL/6 mice (average weight, approximately 23 g) were used for all experiments, with the exception of the model of hyperacute shock (see below) in which female mice were used. All mice were kept on a standard diet and a 12-h day/night rhythm. RIPK3-deficient mice were obtained from V. Dixit (Genentech, La Jolla, CA) (2). Cyclophilin (Cyp)D-deficient mice and SCID-Beige mice were purchased from The Jackson Laboratory, and C57BL/6 mice were from Charles River. Genotypes were confirmed by tail-snip PCR using the following primers: RIPK3: RIPK3-1 (reverse), CGCTTA-GAACCTTCAGGTTGAC; RIPK3-2 (forward-I), GCCTG-CCCATCAGCAACTC; RIPK3-3 (forward-II), CCAGAGGCC-ACTTGTGTAGCG; CypD: 8584 [wild-type (wt) forward], CT-CTTCTGGCAAGAATTGC; 8585 (reverse, common), ATT-GTGGTTGGTGAAGTCGCC; 8586 [knockout (ko) forward], GGCTGCTAAAGCGCATGCTCC; caspase-8: C8-1, CCAGG-AAAAGATTGTGTCTA; C8-2, GGCCTTCCTGAGTACTG-TCACCTGT. All in vivo experiments were performed according to the *Protection of Animals Act* after approval of the German local authorities or the Institutional Animal Care and Use Committee (IACUC) of the University of Michigan and the National Institutes of Health *Guidelines for the Care and Use of Laboratory Animals* after approval from the University of Michigan IACUC. In all experiments, mice were carefully matched for age, sex, weight, and genetic background.

Isolation of Renal Tubules. Six to twelve mice were used for each isolated tubule preparation, depending on the amount of material needed for particular experiments. For preparation of isolated tubules, mice were anesthetized with ketamine (100 mg/kg i.p.) and xylazine (10 mg/kg i.p.), and the kidneys were immediately removed. Type I collagenase was from Worthington Biochemical. Percoll was purchased from Amersham Biosciences. All other reagents and chemicals, including delipidated BSA (catalog no. A6003) were of the highest grade available from Sigma-Aldrich. Immediately after removal of the kidneys, the parenchyma was injected with 0.3–0.5 cc of a cold 95% O₂/5% CO₂-gassed solution consisting of 115 mM NaCl, 2.1 mM KCl, 25 mM NaHCO₃, 1.2 mM KH₂PO₄, 2.5 mM CaCl₂, 1.2 mM MgCl₂, 1.2 mM MgSO₄, 25 mM mannitol, 2.5 mg/mL fatty acid free BSA, 5 mM glucose, 4 mM sodium lactate, 1 M alanine, and 1 mM sodium butyrate (solution A) with the addition of 1 mg/mL collagenase (type I; Worthington Biochemical). The cortices were then dissected and minced on an ice-cold tile and then resuspended in additional solution A for 8–10 min of digestion at 37 °C, followed by enrichment of proximal tubules using centrifugation on self-forming Percoll gradients. For TNF, TWEAK, and IFN- γ (TTI) studies in renal tubules, renal cortices were dissected in ice-cold dissection solution (DS) [HBSS with 10 mmol/L glucose, 5 mmol/L glycine, 1 mmol/L alanine, 15 mmol/L Hepes (pH 7.4); osmolality, 325 mOsmol/L] and sliced into 1-mm pieces. The fragments were transferred to collagenase solution (DS with 0.1% wt/vol type 2 collagenase and 96 μ g/mL soybean trypsin inhibitor) and digested for 30 min at 37 °C and 850 rpm. After digestion, the supernatant was sieved through two nylon sieves, first 250- μ m pore size and then 100- μ m pore size. The longer proximal tubule segments remaining in the 100 μ m sieve were resuspended by flushing the sieve in the reverse direction with warm DS (37 °C) containing BSA 1% (wt/vol). The proximal tubule suspension was centrifuged for 5 min at 170 \times g, washed, and then resuspended into the appropriated amount of culture medium (1:1 DMEM/F12 without phenol red and supplemented with heat-inactivated 1% FCS, 15 mmol/L Hepes, 2 mmol/L L-glutamine, 50 nmol/L hydrocortisone, 5 μ g/mL insulin, 5 μ g/mL transferrin, 5 ng/mL sodium selenite, 0.55 mmol/L sodium pyruvate, 10 mL/L 100 \times nonessential amino acids, 100 IU/mL penicillin, and 100 μ g/mL streptomycin buffered to pH 7.4; osmolality of 325 mOsmol/kg H₂O). The proximal tubule fragments were seeded onto tissue culture plate and cultured at 37 °C and 95% air/5% CO₂ in a standard humidified incubator.

Experimental Procedures for Isolated Tubules. Incubation conditions were similar to those used previously for mouse tubule studies (3). Tubules were suspended at 2.0–3.0 mg of tubule protein per milliliter in a 95% air/5% CO₂-gassed medium containing (in mM) 110 NaCl, 2.6 KCl, 25 NaHCO₃, 2.4 KH₂PO₄, 1.25 CaCl₂, 1.2 MgCl₂, 1.2 MgSO₄, 5 glucose, 4 sodium lactate, 0.3 alanine, 5 sodium butyrate, 2 glycine, and 1.0 mg/mL bovine gelatin (75 bloom) (solution B). For studies comparing normoxia with hypoxia/reoxygenation, at the end of the 15 min, preincubation tubules were resuspended in fresh solution B and regassed with either 95% air/5% CO₂ (normoxic controls) or 95% N₂/5% CO₂ (hypoxia). During hypoxia, solution B was kept at pH 6.9 to simulate tissue acidosis during ischemia in vivo and the usual substrates (glucose, lactate, alanine, and butyrate) were omitted. After 30 min, samples were removed for analysis. The remaining tubules were pelleted and then resuspended in fresh 95% air/5% CO₂-gassed, pH 7.4 solution B with experimental agents as needed. Sodium butyrate in solution B was replaced with 2 mM

heptanoic acid during reoxygenation and supplemented with 250 μ M AMP, 0.5 mg/dL delipidated albumin, and 4 mM each α -ketoglutarate and malate. After 60 min of reoxygenation, tubules were sampled for studies.

Lactate dehydrogenase release assay. Lactate dehydrogenase (LDH) activity was measured before and after the addition of 0.1% Triton X-100 as described previously (4).

Tubule staining with H33342, PI, and TUNEL. At the end of the desired experimental period, 5 μ g/mL H33342 and 3 μ g/mL propidium iodide were added to an aliquot of tubules. After 90 s, the tubules were pelleted and either resuspended in an ice-cold solution containing (in mM) 110 NaCl, 25 Na-Hepes (pH 7.2), 1.25 CaCl₂, 1.0 MgCl₂, 1.0 KH₂PO₄, 3.5 KCl, 5.0 glycine, and 5% polyethylene glycol (average molecular weight of 8,000) for immediate viewing or fixed in 4% paraformaldehyde for later examination. TUNEL assays were performed using the In Situ Cell Detection Kit, TMR red (Roche Diagnostic) according to the manufacturer's instructions. Cytospinning for 10 min at 1,500 rpm [low acceleration with Cytospin 2 (Shandon)] was performed before TUNEL staining. Nuclei were visualized using 4',6-diamidino-2-phenylindole staining (Dianova). Stained sections were analyzed using an Axio Imager Z1 microscope (Zeiss) at 200 \times magnification. Micrographs were digitalized using an AxioCam MRm camera and AxioVision Version 4.8 software (Zeiss). Cell death rate was quantified from five different areas of the slides as a ratio of DAPI and TUNEL double-positive nuclei/DAPI-positive nuclei.

TTI Assay in Tubules. Primary proximal tubules were cultured in 24-well plates at 37 °C and 95% air/5% CO₂ in a standard humidified incubator. They were treated with 25 μ M zVAD and/or 25 μ M Nec-1 for 30 min before the addition and further incubation of 5.5 h with 100 ng/mL recombinant TNF α , 200 ng/mL TWEAK, and 100 U/mL IFN- γ . DMSO was accordingly added to achieve the final vehicle concentration of 7.5 μ L/mL in each well.

Fluorescence-Activated Cell Sorting. Phosphatidylserine exposure to the outer cell membrane of apoptotic cells or at the inner plasma membrane of necrotic cells and incorporation of 7-AAD into necrotic cells was quantified by fluorescence-activated cell sorting (FACS) analysis. The ApoAlert annexin V–FITC antibody and the 7-AAD antibody were purchased from BD Biosciences. The MitoProbe Transition Pore Assay Kit (Invitrogen) was used for detection of mitochondrial permeability transition (MPT) opening and was used according to the manufacturer's instructions. Fluorescence was analyzed using an FC-500 (Beckman Coulter) flow cytometer.

Histology, Immunohistochemistry, and Evaluation of Structural Organ Damage. Organs were dissected as indicated in each experiment and infused with 4% neutral-buffered formaldehyde, fixated for 48 h, dehydrated in a graded ethanol series and xylene, and finally embedded in paraffin. Paraffin sections (3–5 μ m) were stained with periodic acid-Schiff (PAS) reagent, according to standard routine protocol. Immunohistochemistry for RIP1 was performed as described previously at a dilution of 1:500 (5). Stained sections were analyzed using an Axio Imager microscope (Zeiss) at 400 \times magnification. Micrographs were digitalized using an

AxioCam MRm Rev. 3 FireWire camera and AxioVision Version 4.5 software (Zeiss). Organ damage was quantified by two experienced pathologists in a double-blind manner on a scale ranging from 0 (unaffected tissue) to 10 (severe organ damage). For the scoring system, tissues were stained with PAS, and the degree of morphological involvement in renal failure was determined using light microscopy. The following parameters were chosen as indicative of morphological damage to the kidney after ischemia–reperfusion injury (IRI): brush border loss, red blood cell extravasation, tubule dilatation, tubule degeneration, tubule necrosis, and tubular cast formation. These parameters were evaluated on a scale of 0–10, which ranged from not present (0), mild (1–4), moderate (5–6), severe (7–8), to very severe (9–10). Each parameter was determined on at least four different animals, with the exception of Fig. S9 in which only two different animals were scored.

Mouse Model of Cisplatin-Induced Acute Kidney Injury. Induction of acute kidney injury (AKI) following cisplatin application has been described previously. Briefly, cisplatin-induced AKI was induced by intraperitoneal application of 20 mg of cisplatin per kilogram of body weight. All mice received a total volume of 200 μ L of PBS with or without 10 mg of zVAD-fmk per kilogram of body weight or 1.65 mg of Nec-1 per kilogram of body weight 15 min before the injection of cisplatin. All groups in which Nec-1 was applied required repeated Nec-1 injection intraperitoneally every 12 h over the first 5 d. When mice in one group were treated with Nec-1, all other groups in the compared groups received PBS of equal volume as repeated injections (this was the case in Figs. S2C and S4E). Blood samples were taken under anesthesia with 99% diethylether (Roth) by retroorbital bleeding, and serum levels of urea and creatinine were determined according to clinical standards in the central laboratory of the University Hospital Schleswig-Holstein, Campus Kiel, Germany, using an enzymatic UV test for urea (Hitachi Modular; Roche) and an enzymatic peroxidase-dependent test for creatinine according to the manufacturer's instructions (Hitachi Modular; Roche).

Mouse Model of Hyperacute zVAD-fmk/TNF α -Induced Shock. The model of zVAD-fmk/TNF α -induced hyperacute shock has been described in detail previously (6) and was used with slight changes. Briefly, 8- to 10-wk-old male C57BL/6, RIPK3-ko, or CypD-ko mice received intraperitoneal injections of 10 mg of zVAD per kilogram of body weight in a total volume of 200 μ L per mouse 15 min prior rapid intravenous injection of 25 μ g of murine TNF α in 200 μ L of PBS via the tail vein. Animals were under permanent observation, survival was checked every 15 min, and overall survival was analyzed.

Statistics. For all experiments, differences of datasets were considered statistically significant when *P* values were lower than 0.05, if not otherwise specified. Statistical comparisons were performed using the two-tailed Student *t* test. Asterisks are used in the figures to specify statistical significance (**P* < 0.05; ***P* < 0.02; ****P* < 0.001). *P* values in survival experiments (Kaplan-Meier plots) were calculated using GraphPad Prism Version 5.04 software. Statistics are indicated as SD (not to SEM).

1. Gerlach B, et al. (2011) Linear ubiquitination prevents inflammation and regulates immune signalling. *Nature* 471(7340):591–596.
2. Newton K, Sun X, Dixit VM (2004) Kinase RIP3 is dispensable for normal NF-kappa B β s, signaling by the B-cell and T-cell receptors, tumor necrosis factor receptor 1, and Toll-like receptors 2 and 4. *Mol Cell Biol* 24(4):1464–1469.
3. Park JS, Pasupulati R, Feldkamp T, Roeser NF, Weinberg JM (2011) Cyclophilin D and the mitochondrial permeability transition in kidney proximal tubules after hypoxic and ischemic injury. *Am J Physiol Renal Physiol* 301(1):F134–F150.
4. Weinberg JM, Davis JA, Abarzua M, Kiani T (1989) Relationship between cell ATP and glutathione content and protection by glycine against hypoxic proximal tubule cell injury. *J Lab Clin Med* 113:612–623.
5. Zhang H, et al. (2011) Functional complementation between FADD and RIP1 in embryos and lymphocytes. *Nature* 471(7338):373–376.
6. Linkermann A, et al. (2012) Dichotomy between RIP1- and RIP3-mediated necrosis in tumor necrosis factor- α -induced shock. *Mol Med* 18:577–586.

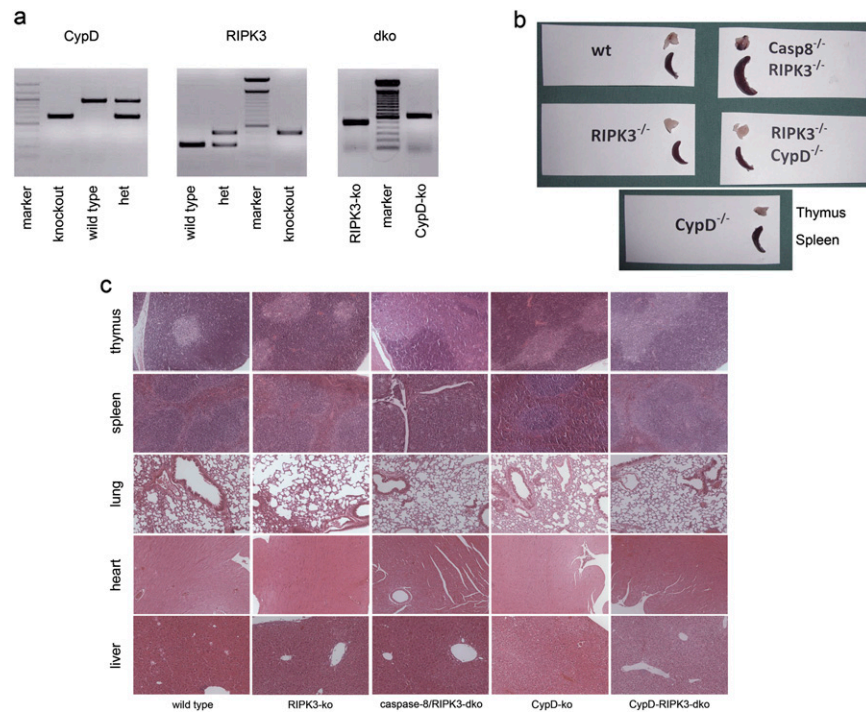


Fig. S1. Characterization of CypD-RIPK3 double-deficient mice. (A) Genotyping for CypD-RIPK3 double (d) ko mice. (B) Comparison of thymus and spleen from wt, RIPK3-ko, CypD-ko, caspase-8-RIPK3-dko, and CypD-RIPK3-dko mice at an age of 8 wk. No splenomegaly was seen in the CypD-RIPK3-ko animals (C) Histological comparison of indicated organs taken from 10-wk-old C57BL/6 wt mice, CypD-ko mice, RIPK3-ko mice, and CypD-RIPK3-dko mice. Histological evaluation did not detect differences in organ architecture.

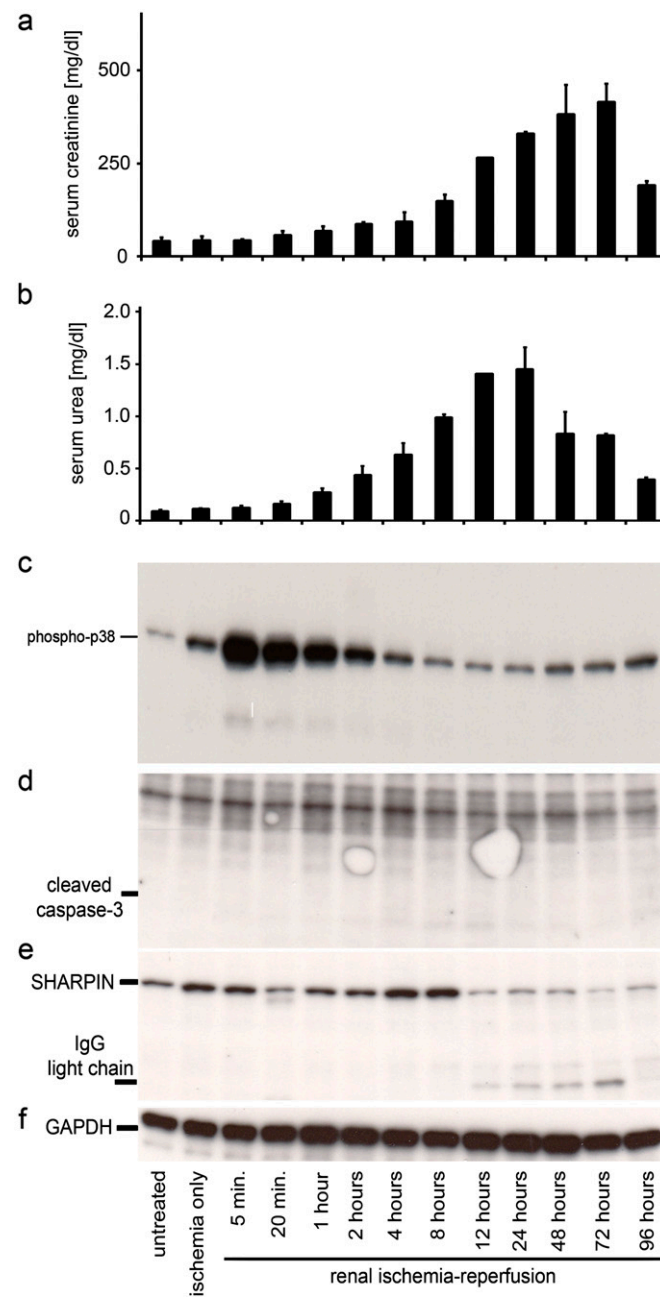


Fig. S2. In vivo time course of cell death regulators in IRI-treated wt mice. Time course of bilateral IRI in 10-wk-old C57BL/6 mice that underwent 30 min of bilateral pedicle clamping followed by different times of reperfusion. Serum creatinine (*A*) and serum urea (*B*) concentrations indicate the renal function and the level of intoxication of mice at each time point, respectively, indicating the severity of renal failure. (*C*) The survival marker p38 underwent phosphorylation within the ischemic phase and was strongly phosphorylated at the beginning of reperfusion. (*D*) In line with previously published data, apoptosis and caspase-3 cleavage is of minor importance in IRI (1, 2). (*E*) SHARPIN, a component of the linear ubiquitinylating complex that regulates RIPK1 polyubiquitination and, thereby, prevents formation of the pronecrotic complex II, is down-regulated during IRI. (*F*) GAPDH serves as a loading control. *n* = 5 mice per group.

1. Kung G, Konstantinidis K, Kitsis RN (2011) Programmed necrosis, not apoptosis, in the heart. *Circ Res* 108(8):1017–1036.
2. Linkermann A, et al. (2012) Rip1 (receptor-interacting protein kinase 1) mediates necroptosis and contributes to renal ischemia/reperfusion injury. *Kidney Int* 81(8):751–761.

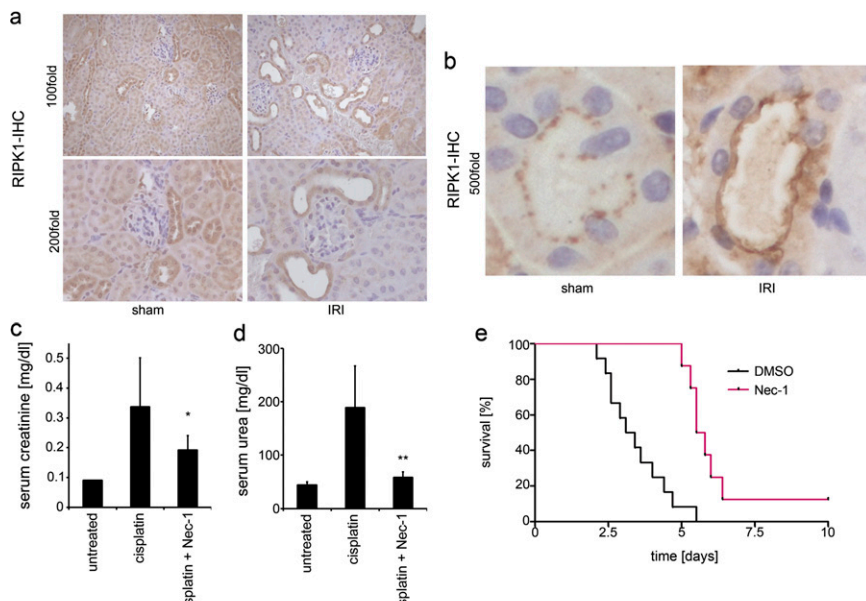


Fig. S3. RIPK1 in AKI. (A and B) Changes in the distribution of RIPK1 in immunohistochemically stained kidney sections from mice that underwent sham surgery or IRI 48 h before fixation. Arrows indicate dilation of renal tubules, a typical sign of severe injury that is associated with IHC positivity for RIPK1. (C–E) Ten-week-old C57BL/6 mice underwent intraperitoneal treatment with vehicle or 20 mg of cisplatin per kilogram of body weight. All mice received 200 μ L of total volume (DMSO or 1.65 mg of Nec-1 per kilogram of body weight) every 12 h. (C and D) Concentrations of serum creatinine and urea are depicted 48 h after cisplatin injection. (E) Overall survival of vehicle-treated (DMSO; $n = 12$) or Nec-1–treated mice ($n = 8$) after cisplatin application.

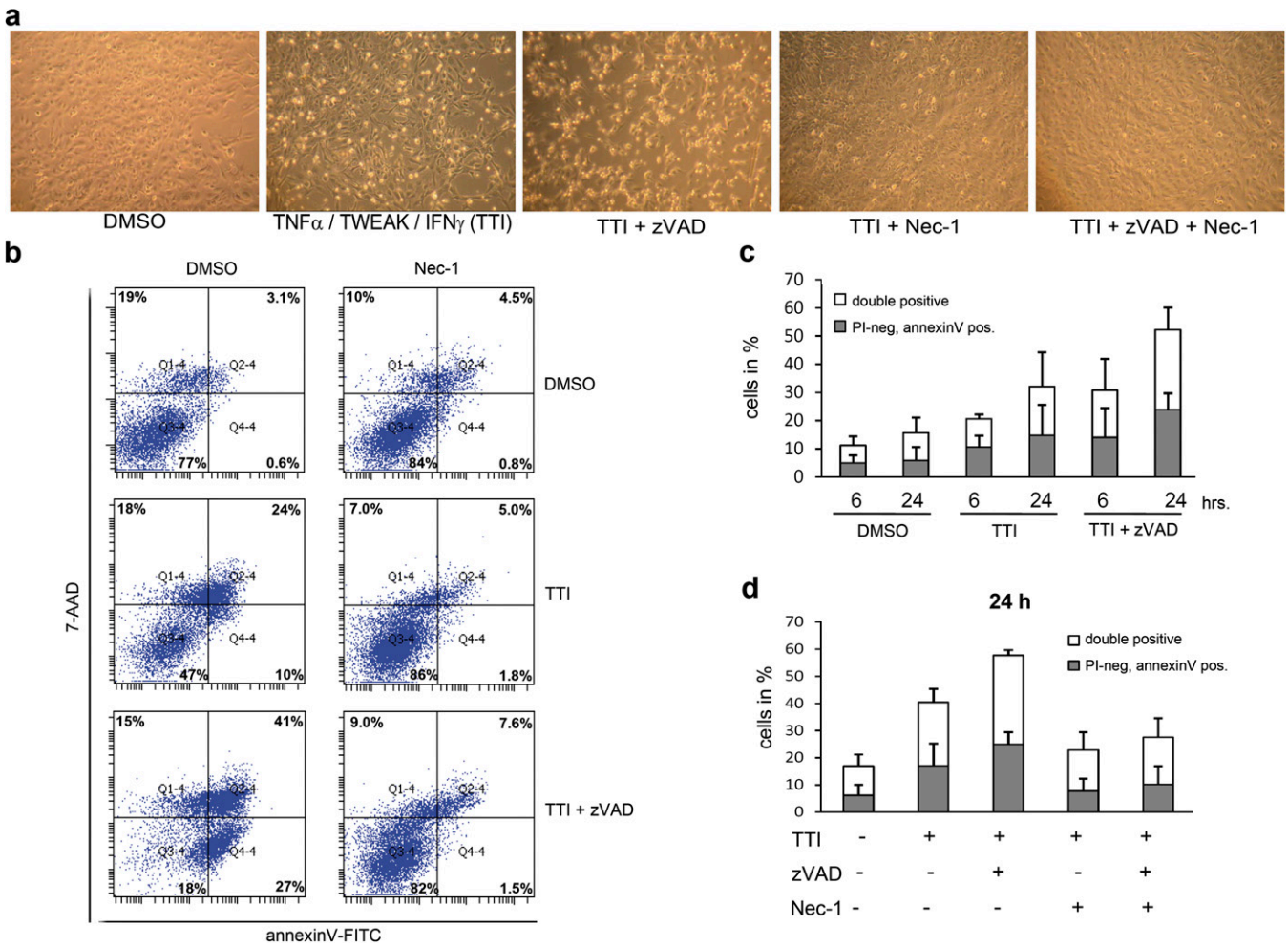


Fig. S4. Detection of necroptosis in the MCT cells. (A) MCT cells were cultured for 24 h in the presence of 30 ng/mL TNF α , 100 ng/mL TWEAK, 30 U/mL IFN γ , 25 μ M zVAD-fmk (zVAD), and 30 μ M Nec-1 as indicated. (B) MCT cells were treated with vehicle (DMSO), TNF α , TWEAK, IFN- γ , zVAD, and Nec-1 for 24 h as indicated before positivity for annexin V and 7-AAD was detected by FACS analysis. (C) MCT cells were treated for 6 or 24 h with either vehicle (DMSO) or the combination of TNF α /TWEAK/IFN- γ (TTI) in the presence and absence of zVAD before evaluation by FACS. Fractions of 7-AAD and annexin V double-positive cells and 7-AAD-negative, annexin V-positive cells are shown. (D) MCT cells were treated for 24 h with indicated reagents incl. Nec-1 and are demonstrated in analogy to C.

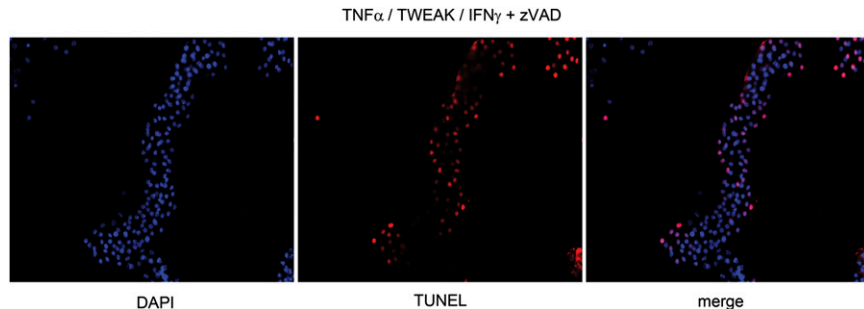
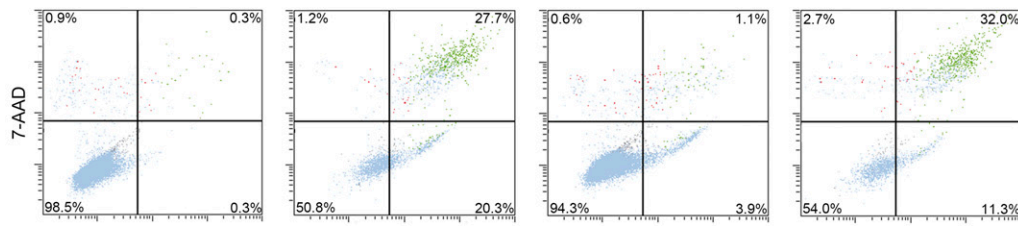


Fig. S5. Caspase-independent cell death in renal tubules. Higher magnification and resolution of the experiment shown in Fig. 3A, exemplified by showing the results of the TTI-zVAD sample.

a



b

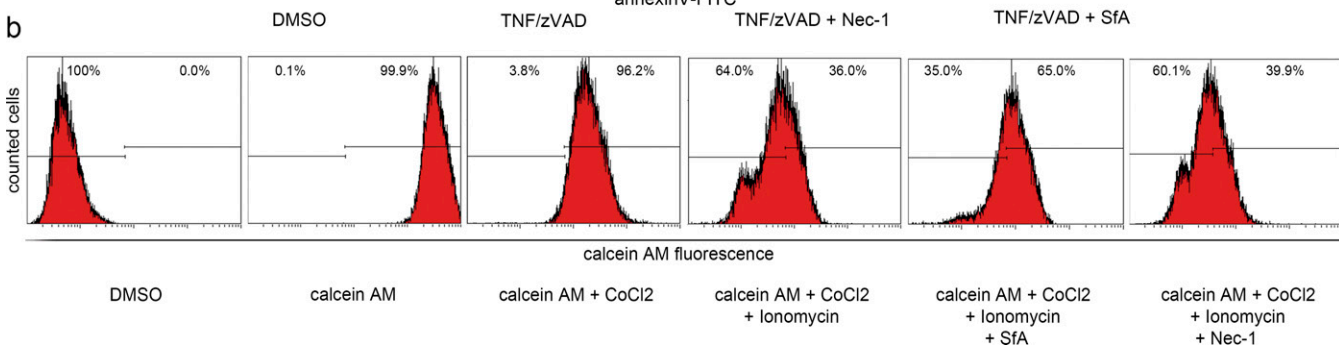


Fig. S6. CypD-dependent regulated necrosis and RIPK3-dependent necroptosis are two distinct cellular response mechanisms. (A) L929 cells were treated for 4 h with the indicated reagents including SfA at a concentration of 5 μ M. Classical necroptosis in the TNF α /zVAD-treated group is prevented by Nec-1 but not by SfA. (B) Calcein AM fluorescence assay with Jurkat cells for the evaluation of MPT pore opening. Fluorescence levels shift upon addition of ionomycin, indicating MPT-pore opening. Whereas SfA potently prevents this shift, no alteration could be detected upon addition of Nec-1.

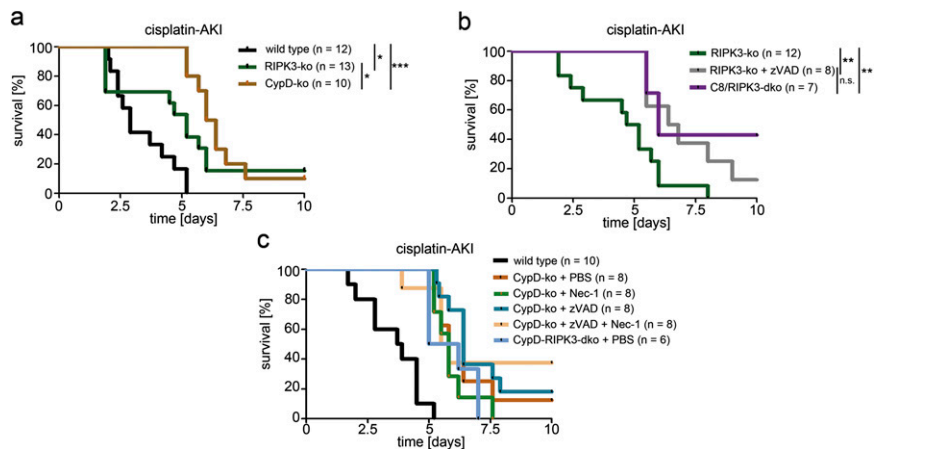


Fig. S7. CypD-dependent regulated necrosis and RIPK3-dependent necroptosis are two distinct cellular response mechanisms. Mice received 20 mg of cisplatin per kilogram of body weight as in Fig. S3 B–D. (A) Both RIPK3-deficient and CypD-deficient mice are significantly protected compared with wt mice. However, the extent of protection of CypD-deficient mice was significantly higher than that of RIPK3-ko mice. (B and C) Whereas RIPK3-deficient mice showed prolonged survival upon addition of zVAD or on the combined genetic background of caspase-8/RIPK3, the protection of CypD-ko mice could not be significantly extended by addition of zVAD, Nec-1, the combination of both, or the combined deficiency of CypD and RIPK3. *P < 0.05; **P < 0.01; ***P < 0.001 (n is indicated for each group).

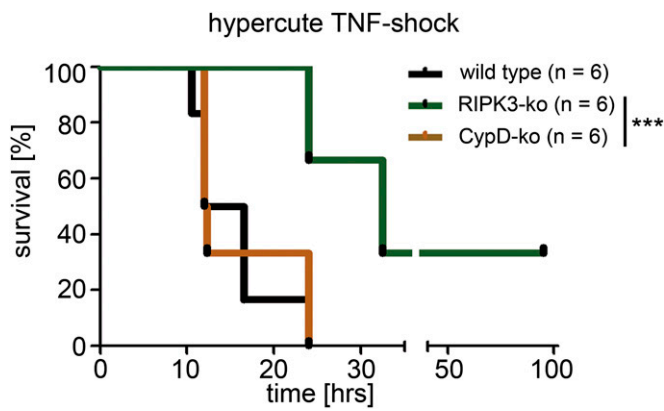


Fig. S8. RIPK3 deficiency protects from hyperacute TNF α -mediated shock, whereas CypD deficiency does not. The model of hyperacute TNF α shock was performed as published previously (1, 2). All mice (10-wk-old female C57BL/6 wt mice, RIPK3-ko mice, and CypD-ko mice) received intravenous injection of 25 mg of murine TNF α 15 min after peritoneal injection of 10 mg of zVAD per kilogram of body weight. In line with the previously published data, RIPK3-deficient mice were protected from hyperacute shock, whereas CypD-ko mice did not show any protection in comparison with wt mice. *** $P < 0.001$ (n is indicated for each group).

1. Cauwels A, Janssen B, Waeytens A, Cuvelier C, Brouckaert P (2003) Caspase inhibition causes hyperacute tumor necrosis factor-induced shock via oxidative stress and phospholipase A2. *Nat Immunol* 4(4):387–393.
2. Linkermann A, et al. (2012) Dichotomy between RIP1- and RIP3-mediated necroptosis in tumor necrosis factor- α -induced shock. *Mol Med* 18:577–586.

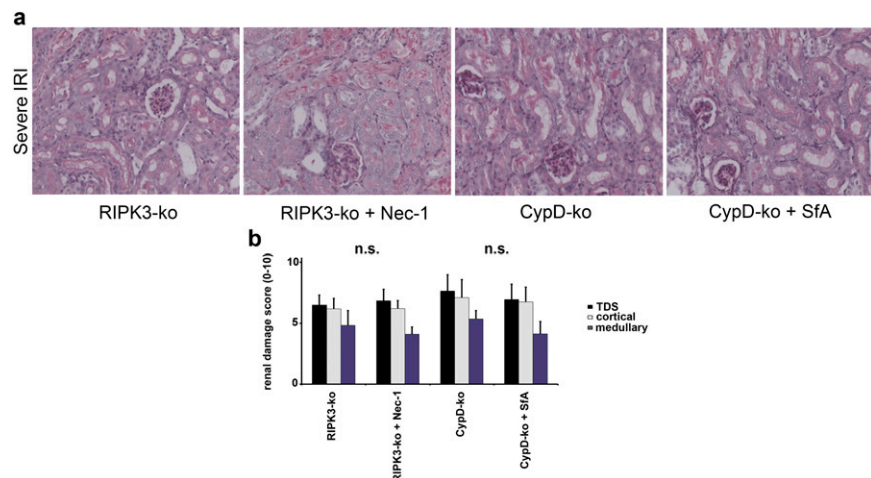


Fig. S9. Specificity of Nec-1 for necroptosis and SfA for CypD-mediated regulated necrosis. (A and B) RIPK3-ko and CypD-ko mice ($n = 8$ per group) underwent indicated treatment 15 min before onset of IRI surgery. Note that the neither the addition of Nec-1 to RIPK3-ko mice nor the application of SfA in CypD-ko mice led to any further protection compared with the DMSO-treated knockouts. Representative PAS-stained histomicrographs (A) and histological quantification by using the renal damage score (B) are demonstrated. n.s., not significant.